Geochemistry International, Vol. 41, No. 4, 2003, pp. 395–409. Translated from Geokhimiya, No. 4, 2003, pp. 443–458.

Mechanism of Chlorine Dissolution in Water-Saturated Model Granodiorite Melt: Applications of IR Spectroscopic Methods

V. Yu. Chevychelov, A. G. Simakin, and G. V. Bondarenko

Institute of Experimental Mineralogy, Russian Academy of Sciences, Chernogolovka, Moscow oblast, 142432 Russia; e-mail: chev@iem.ac.ru

Received July 3, 2001

Abstract—The joint solubility of Cl and H_2O was experimentally studied at P = 1 kbar and T = 1000°C in a model granodiorite melt interacting with water–salt fluid within a wide range of bulk fluid concentration, from 0 to ~98 wt % of chlorides. The structure of granodiorite melts was characterized on the basis of the IR spectra of quenched glasses. Total water content and concentrations of various water species (H_2O_{mol} and OH^-) were determined in the same glasses by the methods of near FTIR spectroscopy. The influence of variations in the concentrations of alkali and alkali earth cations, chlorine, and water on the structure of medium-range order in granodiorite glass was evaluated.

INTRODUCTION

The investigation of the solubility of various components of natural fluids such as chlorine and fluorine in granite and granodiorite melts is important for the modeling of ore systems. Ore systems dominated by fluorides and chlorides differ both in the characteristics of the geologic environments of their formation and evolution and in their affinity to particular metals [1, 2]. The differences of the fluoride and chloride paths of magma evolution are largely related to differences in the nature of interaction of these halogens with magmatic melts.

Chlorine solubility in acid aluminosilicate melts has been repeatedly studied in experiments as a function of various physicochemical factors and was comprehensively reviewed by Malinin and Kravchik [3], Webster [4], and Chevychelov [5].

The problem of the effect of high fluid salinity on the solubility of chlorine in melt is not adequately understood, because most investigations were concerned with solutions with Cl concentrations no higher than 6–8 m. A significant increase in chlorine solubility in albite–quartz eutectic melt was reported in the region of high chlorine concentration in fluid (82 wt % NaCl), up to ~1.8 wt % in comparison with ~0.25% at an NaCl concentration in fluid of <50% at 1.5 kbar and 900°C [3].

Shinohara *et al.* [6] demonstrated that at low pressures of 0.6 and 1.2 kbar and 810°C, the chloride concentration of granite melt is constant and independent of the "bulk" Cl abundance in fluid phases within a wide field of water vapor–chloride liquid immiscibility. On the other hand, at pressures from 2.2 to 6.0 kbar, the chlorine content of granite melt increases continuously with increasing concentration of the coexisting homogeneous aqueous chloride solution [6].

Webster [4, 7–9] investigated the joint concentration of Cl and H_2O in aluminosilicate melts of granite, andesite, and basalt compositions both under water-saturated and water-undersaturated conditions at pressures of 2.0, 0.5, and 0.001 kbar. He revealed a general decrease in the Cl concentration of melt with increasing H_2O activity in the system. According to Webster [7, 10], at varying P–T conditions and compositions, two types of combined Cl and H_2O concentration operate in aluminosilicate melt. (1) At relatively high temperature and low pressure, aqueous chloride fluid is characterized by a rather wide miscibility gap. In the presence of homogeneous low-concentration fluid, an increase in the content of chloride in the system results in rapid Cl accumulation in aluminosilicate melt at constant H_2O content. In the domain of the two-phase fluid, the concentrations of Cl and H_2O in aluminosilicate melt reach maximum values and remain approximately constant. A further increase in chloride content and transition of the fluid into a homogeneous highly concentrated fluid–melt result in the depletion of aluminosilicate melt in H_2O at constant Cl content. (2) The second type of combined Cl and H_2O concentration in aluminosilicate melt is observed in the region of higher pressure and low temperature beyond the fluid immiscibility field. In this case, the Cl concentration of the melt coexisting with homogeneous aqueous chloride fluid increases gradually and that of H_2O decreases with increasing bulk Cl abundance in the system.

Webster [9] has also considered possible changes in Cl and H_2O contents in residual aluminosilicate melt and fluid phases separated in the course of various magmatic processes. (1) For instance, Cl and H_2O gradually

accumulate in residual melt during the eutectic crystallization of quartz and feldspar from volatile-undersaturated haplogranite melt. (2) In the case of isobaric crystallization of volatile-saturated aluminosilicate melt, the behavior of Cl and H_2O depends on the phase state of the released fluid. The concentrations of Cl and H_2O in the residual melt are either inversely proportional to each other (one fluid phase) or nearly constant and close to the maximum values (two fluid phases). (3) In the case of decompression degassing of volatile-saturated melt, H_2O content in the residual melt may vary strongly depending on P_{final}, whereas variations in chlorine content are relatively small.

Unfortunately, there is almost no evidence in the literature on the structure of chlorine-bearing melt obtained by modern spectral methods and investigations of the mechanism of chlorine dissolution in hydrous aluminosilicate melts. It is known that network-forming elements, mainly silicon and aluminum, are tetrahedrally coordinated to four oxygen atoms in aluminosilicate melts at moderate pressure. The structure of silicate melt is classified at the lowest (initial) level (short-range order) depending on the degree of bonding of tetrahedra through a common oxygen atom, which is known as Q specification [11]. It is based on the types (bridging or nonbridging) of oxygen atoms surrounding Si or Al. The structures vary from the maximum degree of bonding, Q_4, when one tetrahedron is connected to four others, to free tetrahedra, Q_0. The distribution of tetrahedra is not uniquely defined by composition because of the possible disproportionation of medium-bonded Q_3 species into polymerized Q_4 and linearly bonded Q_2 species. The proportions of these species can be successfully estimated from the analysis of IR spectra in the region of deformation vibrations 850–1600 cm^{-1} [11, 12].

In this study, we used another approach and described the structure of melt in the context of the structure of medium-range order. The medium-range order concerns the sphere of the nearest neighbors that form the minimum closure. In general, this approach is independent of the Q specification. Previously, we characterized the structure of medium-range order in melts [13] as a size distribution of the smallest topologically indecomposable aluminosilicate rings (topological term) [14]. The size varies within a narrow range: three-, four-, and six-membered rings have been established. Four- and six-membered rings are typical structural elements of silicate minerals. Rings made up of tetrahedra are distorted to a varying extent because of their closing. They are characterized therefore by individual T–O–T angles, which are recorded in deformation vibrations (T denotes Si and Al, network-forming element; O is oxygen).

The most distorted three-membered rings have the highest frequency (absorption band) at 600 cm^{-1}. Three-membered rings were detected in strongly polymerized melts (NBO/T = 0) containing anorthite. They are almost absent in hydrous silicic melts. The existence of five-membered rings remains to be demonstrated. They were never found in tectosilicate minerals. However, in the context of statistics and formal topology, they must occur. This was suggested, for example, in the interpretation of X-ray data by Zotov [15]. On the other hand, while four-membered rings show a distinct individual absorption band at 460 cm^{-1} (anorthite melt), and six-membered rings, at 400–420 cm^{-1} (tridymite melt), no absorption band due to five-membered rings was ever found. Strictly speaking, there must be a preference for four- and six-membered ring sizes because of the selectivity of chemical interaction of network-modifying cations (Na, Ca, and K) with the aluminosilicate network. In this sense, it is possible to consider end-members, i.e., chemical compounds, in melt. Our interpretation of the structure of medium-range order in melts is not rigorously substantiated, because there exists a formal possibility of the detection of the third absorption band corresponding to five-membered rings. In this respect, it is possible to consider the apparent (effective) size distribution of the smallest topologically indecomposable aluminosilicate rings.

Our interpretation of spectral data is supported by the good correlation between the calculated proportion of rings in the *Ab–An* system and glass composition [13]. Simakin *et al.* [13] also studied the influence of water on the character of ordering of the structure of granite melt using the method of IR absorption spectroscopy. It was found that the fraction of six-membered aluminosilicate rings increased with increasing H_2O content.

In this paper, we attempted to apply our recently developed methods to the analysis of the effect of water and chlorine dissolved in granodiorite melt on the structure of medium-range order in the melt. In such a way, we intended to elucidate the mechanism of chlorine dissolution.

EXPERIMENTAL AND ANALYTICAL METHODS

Starting Materials, Preparation, and Conditions of Experiments

The initial glass modeled granodiorite composition (wt %, calculated): 68.4 SiO_2, 17.9 Al_2O_3, 5.2 CaO, 4.0 Na_2O, and 4.5 K_2O was prepared from gel. The gel mixture was obtained by the procedure described in [16, 17]. In most cases, nitrates were used as initial salts. The final temperature of annealing was 600°C. Aluminosilicate glasses were prepared initially by "dry" melting of gel at $P \sim 1$ bar, a stepwise temperature increase from 700 to 1360°C, and a run duration of about three days. The melt was exposed at $T \geq 1300$°C for about one day. The powdered glasses were subsequently melted under "hydrothermal" conditions at $P_{tot} = P_{H_2O} = 1$ kbar, $T = 1100$°C, a run duration of

about one day, and f_{O_2} close to the Ni–NiO buffer. A column of the hydrous glass obtained was sectioned by a thin diamond saw into pieces (~30–90 mg), which were used in the experiments on solubility determination. For experiments 234 and 235, *optically bubble-free* water-saturated glass was specially prepared. For this purpose, air was expelled before the melting of powdered glass and replaced by water, i.e., a liquid mush consisting of approximately equal amounts of powdered glass and H_2O was loaded into the ampoule.

Experiments on the investigation of chlorine solubility in hydrous granodiorite melt were conducted at $P_{tot} = P_{H_2O} = 1 \pm 0.1$ kbar, $T = 1000 \pm 10$°C, and a duration of four days in internally heated high-pressure gas vessels (UVGD-10000). Experiment 240 was carried out at $T = 1050$°C in order to produce a clear glass devoid of crystalline phases. The high temperature of the experiments was dictated by the high liquidus temperature of the melt [5], which contained initially 5.2 wt % CaO. Chevychelov [5] demonstrated that an experimental duration of four days was sufficient under such *P–T* parameters for the attainment of near-equilibrium conditions. This is indirectly supported by the absence of differences in the concentrations of chlorine and major components in the marginal and central parts of samples of aluminosilicate glass after experiments.

For a given fluid composition, a chloride solution and a mixture of chemical reagents was also loaded into the ampoule. We used ~1 *n* Cl solution of the following composition: 0.05 *n* HCl + 2.4 wt % NaCl + 2.2 wt % KCl + 0.9 wt % $CaCl_2$ + 0.49 wt % $AlCl_3 \cdot 6H_2O$, and the chemical reagents NaCl, KCl, $CaCl_2$ (molten), $AlCl_3 \cdot 6\ H_2O$, and amorphous SiO_2. The weight proportions of particular reagents and solution were chosen to minimize changes in the composition of aluminosilicate melt after experiments. In other words, we attempted to reach the minimum differences between the compositions of aluminosilicate melts after experiments at varying chloride content in the fluid with respect to Si, Al, Ca, Na, and K oxides. This allowed us to compare more straightforwardly the results of subsequent spectroscopic investigations. In experiments without initial chlorine, pure tridistilled water and alkalic solutions of the following composition were used: 1.7 wt % KOH + 2.6–5.8 wt % $Na_2SiO_3 \cdot 9H_2O$, together with CaO, Al_2O_3 and amorphous SiO_2.

We believe that chlorine dissolved in the aluminosilicate melt via diffusion from fluid, because in all our experiments, initial glass chips were not powdered and chlorine was introduced into the initial system only with fluid.

Preliminary mixed sodium, potassium, calcium, and aluminum chlorides and amorphous silica were loaded into a platinum ampoule ($6 \times 0.2 \times 25$ mm), whence a piece of aluminosilicate glass wrapped in 0.1-mm-thick platinum foil was inserted, and ~1 *n* ΣCl initial solution was poured in. Each step was controlled by weighing with an accuracy of 10^{-4}–10^{-5} g. In order to eliminate air, the ampoule was blown with argon before welding. The initial weight ratio glass/fluid was from 1.0 to 0.3.

After the experiment, the ampoule was carefully wiped, weighed, and opened. The pH of the quenched solution was measured by universal indicator paper. The quenched glass was rinsed for 10–20 min in tridistilled water with heating up to 80–100°C, then dried and weighed. The weight loss of the aluminosilicate sample due to melt dissolution or the weight gain due to absorption of matter from solution was usually from 0 to ±4% rel.

Each glass sample was carefully divided into two parts using a sharpened piece of corundum. Half of the sample was used for a polished section, which exposed the whole lateral section of the sample, i.e., its central and marginal parts. The polished sections were examined on an optical microscope under reflected light in order to check for the presence of crystalline phases, and the composition of the samples was then determined on an electron microprobe. The second portion of the sample was ground and used for IR spectral investigations. Double-polished thin sections were also prepared from pieces of samples for water analysis.

Electron Microprobe Analysis

The full chemical composition of aluminosilicate glasses was determined after experiments by the method of microprobe analysis on a Camebax microprobe equipped with an energy-dispersive spectrometer Link. The counting time (τ) was 100 s; beam diameter, ~2–5 μm; and $U = 15$ kV. From 6 to 14 measurements were made in each sample in the margins, center, and by moving through the whole sample section. The average contents were then used. In order to minimize sodium and potassium losses, the analysis was conducted with continuous movement of the beam over the sample surface. The analyses of some samples were repeated under different conditions: (a) τ = 400–200 s and (b) scanning over an area of 10×10 μm. Rare crystals occurred in some experiments and were also analyzed. The concentrations were calculated using the ZAF correction procedure. The procedure of chlorine analysis was described in detail by Chevychelov [5].

Infrared Absorption Spectroscopy

The infrared absorption spectra of samples were recorded within a wavenumber interval of 300–800 cm^{-1} in digital form on a Perkin Elmer m.983 spectrophotometer. A routine method was used with pressed KBr tablets containing about 0.4–0.5% of the material studied (~2 mg of powdered sample). For about half of the samples, two or three IR spectra were recorded using materials from different sample portions. The obtained complex wide asymmetric bands of IR spectra in the frequency range 300–600 cm^{-1} were approximated by two symmetric contours related to vibrations of four-

and six-membered aluminosilicate and silicate rings using the program GRAMS for spectrum processing.

FTIR Spectroscopy

In order to determine water content, double-polished plates were prepared from each sample, 110–390 μm thick. Near-IR spectra within 4000–6000 cm^{-1} (in the region of overtone and combination bands) were recorded in Pisa University, Italy, by P. Armienti on an FTIR spectrometer. This method allows the local measurement of IR spectra at a beam diameter of 20–30 μm and selection of a beam path between crystals and bubbles, if the glass is not sufficiently homogeneous. The total water content was determined as a sum of the concentrations of OH groups (band with a maximum at about 4500 cm^{-1}) and molecular water (peak of 5200 cm^{-1}). The calculations were carried out using the formulas [18]

$$C_{H_2O}(\text{wt }\%) = \frac{1802A_{H_2O}}{d\rho\varepsilon_{H_2O}} \quad (1)$$

and

$$C_{OH}(\text{wt }\%) = \frac{1802A_{OH}}{d\rho\varepsilon_{OH}}, \quad (2)$$

where A_{H_2O} and A_{OH} are absorptions in the maxima of the bands due to molecular water and OH groups; ρ is the glass density in g/l; d is the thickness of the glass plate, which was determined directly in the point where the IR spectrum was measured, cm; and ε_{H_2O} and ε_{OH} are the molar extinction coefficients in l/(mol cm). They were calculated after [18] accounting for SiO_2 content in glass samples for the absorption bands of molecular H_2O and OH groups. The correction for the recalculation of OH group content was included in the extinction coefficient. The values of absorption for most samples were measured in two to four widely spaced points.

Measurement of Sample Density

In order to calculate water content in a quenched glass sample from its FTIR spectral characteristics, the density of this glass must be known. Sample density was measured using a TGP-1 thermal gradient device. The method of two standards was used with a mixture of bromoform with a small amount of absolute alcohol as a working liquid. The measurements were carried out by T.V. Prasol. The results are shown in Table 1.

Transmission Electron Microscopy

Samples 222 (0.96% of Cl) and 224 (without Cl) were studied on a transmission electron microscope ICX (TEM) at a magnification of 100 000. The analysis of the powdered samples was carried out by V.I. Nikolaichik in the Institute of Microelectronic Technology and Ultra-High-Purity Materials, Russian Academy of Sciences (Chernogolovka, Moscow oblast). No apparent differences were found between the amorphous matters of these two samples. In the amorphous particles of sample 222, no crystalline phases were found that could have been identified as chlorides. Thus, it is reasonable to suggest that chlorine was homogeneously distributed in our experiments through the volume of aluminosilicate melt.

EXPERIMENTAL RESULTS

Chlorine Solubility in Model Granodiorite Melt

Table 1 presents the experimental results on chlorine solubility in water-saturated model granodiorite melt coexisting with water–salt fluid of a complex composition. The bulk content of chlorides (recalculated to the chloride of a monovalent metal, MeCl) varied in the initial solution within a wide range from 0 to ~98 wt % with an increment of 1–25 wt %. The quenched granodiorite glasses from experiments 217 and 218 appeared to be strongly depleted in calcium because of its extraction into fluid. In subsequent experiments, the use of calcium-rich initial solutions allowed us to minimize changes in the composition of aluminosilicate glasses after experiments. Quenched glasses from some experiments contained plagioclase and, occasionally, quartz crystals, which accounted for no more than 5–10% by volume. According to microprobe analysis, the plagioclase is labradorite (wt %, 53.5 SiO_2, 29.1 Al_2O_3, 13.2 CaO, 3.5 Na_2O, and 0.5 K_2O) or, occasionally, pure anorthite (45.6 SiO_2, 34.7 Al_2O_3, 19.1 CaO, 0.3 Na_2O, and 0.3 K_2O). Fibrous mullite crystals (~27.2 SiO_2 and ~72.8 Al_2O_3) or mixtures of mullite and sillimanite were found in experiment 218.

Figure 1 shows the chlorine content of aluminosilicate melt depending on the bulk chloride abundance in fluid. Under the P–T parameters of our experiments, the system under investigation occurs in the field of two-phase fluid in a rather wide range of chloride contents. This diapason can be roughly estimated to lie between ~1.0–4.5 and ~80–95 wt % [19–21]. Figure 1 displays the fields of low-density vapor (L_1) and salt (L_2) fluids and the field where these two fluids coexist ($L_1 + L_2$). The solubility of chlorine in melt is rather low (0.1–0.5%) in the region of vapor fluid (L_1) but rapidly increases with increasing chlorine content in the system. Within this field, the partition coefficient of chlorine between fluid and melt ($D_{fluid/melt}$) is lower than ten. Chlorine solubility in melt reaches a maximum value of 0.96% in equilibrium with the two-phase fluid at relatively low bulk chloride content in the fluid (~7–11 wt %). At the higher chloride content of fluid, the solubility of chlorine in granodiorite melt decreases slightly to 0.50–0.65 wt % and remains approximately constant in equilibrium with fluid phases with a "bulk" MeCl content of more than ~15 wt %. We did not observe any appreciable increase in the chlorine content of magmatic melt

Table 1. Experimental conditions (T = 1000°C and P = 1 kbar), densities, compositions, and various molar ratios of granodiorite glasses after experiments determined by microprobe analyses

Run no.	$C_{init.\,sol}$, % MeCl[4]*	$pH^{5*}_{quench\ sol}$	$V_{cryst\ phase}$, %[6]*	ρ[7]*, g/cm^3	SiO_2	CaO	Na_2O	K_2O	Al_2O_3	Cl[8]*	A/CNK[9]*	NK/A[9]*	ANC/S[9]*	ANCK/S[9]*
214 (initial)[1]*	–	6	–	–	70.45	4.9	3.6	4.35	16.6	0	0.852	0.638	0.451	0.530
215	–	5	–	–	70.6	4.7	3.6	4.25	16.7	0	0.876	0.630	0.449	0.526
223	–	6	–	–	66.9	5.0	5.4	5.2	17.3	0	0.733	0.839	0.541	0.641
224	–	6	–	2.37	68.1	4.9	4.4	5.45	17.2	0	0.780	0.764	0.500	0.602
228	1.7	1	up to 5% *Pl*	–	69.7	5.2	3.7	4.0	17.1	0.08	0.861	0.609	0.472	0.545
241	3.8	1	–	–	70.15	4.45	4.15	4.45	16.4	0.27	0.831	0.710	0.458	0.539
242	4.8	≤1	–	2.35	69.2	4.5	4.5	5.0	16.1	0.53	0.767	0.796	0.470	0.562
216	7.3	<1	–	–	68.4	4.6	4.5	5.2	16.3	0.86	0.762	0.799	0.480	0.577
222	9.9	<1	–	–	68.0	4.8	4.3	5.1	16.8	0.96	0.788	0.750	0.489	0.585
234 (bubble-free)[2]*	10.9	≤1	–	–	69.0	4.2	4.4	5.2	16.4	0.70	0.800	0.785	0.469	0.565
230	37.3	<1	–	2.33	69.9	2.5	4.7	5.6	16.5	0.55	0.900	0.836	0.447	0.549
231	57.2	<1	5–10% *Pl* + ?*Qtz*	–	70.6	2.7	4.1	5.2	16.7	0.56	0.966	0.741	0.432	0.526
217 (large Ca deficit)[3]*	69.2	<1	?	–	70.8	1.2	4.5	5.6	17.1	0.65	1.093	0.787	0.426	0.527
220	71.0	≤1	5–10% *Pl*	–	71.15	4.1	3.75	3.6	16.95	0.48	0.967	0.594	0.445	0.509
225	75.3	≤1	5–10% *Pl*	–	72.1	3.8	3.4	4.0	16.1	0.58	0.957	0.616	0.411	0.482
218 (large Ca deficit)[3]*	87.1	1	5–10% *Mul–Sil*	–	72.5	0.3	3.7	5.7	16.9	0.78	1.320	0.725	0.378	0.478
235 (bubble-free)[2]*	88.6	2	up to 5% *Pl*	–	72.6	3.6	3.8	4.4	14.9	0.63	0.849	0.739	0.396	0.474
240 (T = 1050°C)	88.7	<1	–	2.33	70.7	3.5	3.8	4.6	16.6	0.75	0.943	0.677	0.434	0.517
221	91.0	5	5–10% *Pl*	–	70.7	4.55	4.7	2.55	16.85	0.62	0.898	0.623	0.479	0.525
227	94.2	–	5–10% *Pl*	–	70.8	4.0	4.0	3.9	16.8	0.33	0.929	0.643	0.450	0.520
244	97.5	?1–1.5	?	2.33	72.3	2.4	3.9	4.8	15.9	0.58	0.994	0.731	0.399	0.484

Note: [1]* Water-saturated aluminosilicate melt, which was directly used in experiments on the investigation of chloride solubility.

[2]* Preliminary molten *optically bubble-free* water-saturated glass was used as initial material.

[3]* Aluminosilicate glass was strongly depleted in calcium after the experiment.

[4]* Calculated total concentration of chlorides in the initial solution expressed as the chloride of a monovalent metal; SiO_2 content is ignored.

[5]* pH of quenched solution measured by universal indicator paper.

[6]* These experimental aluminosilicate glasses contained separate crystals of plagioclase (*Pl*) and, occasionally, quartz (*Qtz*). Fibrous crystals of mullite and a mullite–sillimanite mixture were found in experiment 218.

[7]* Densities ρ of granodiorite glasses were measured after experiments on a TGP-1 thermal gradient device.

[8]* Error in chlorine analysis σ_{C_m} is 0.04–0.06 wt % (see text and [5] for detail).

[9]* Molar ratios: A/CNK = $Al_2O_3/(CaO + Na_2O + K_2O)$, NK/A = $(Na_2O + K_2O)/Al_2O_3$, ANC/S = (Al + Na + Ca)/Si, and ANCK/S = (Al + Na + Ca + K)/Si.

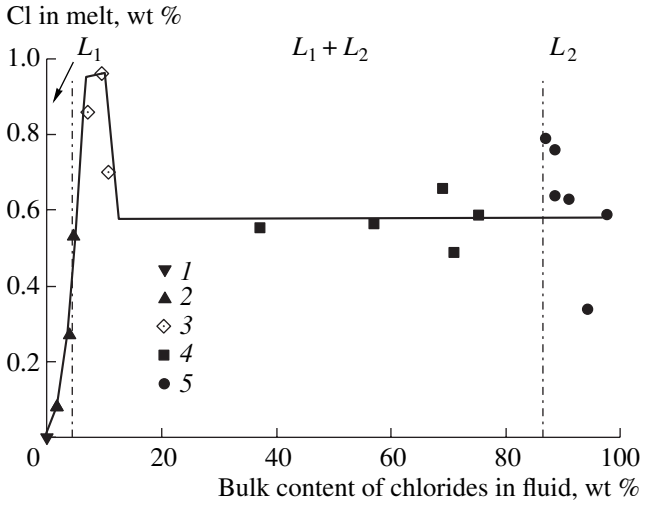

Fig. 1. Chlorine content of granodiorite melt as a function of the bulk chloride abundance of fluid. L_1 and L_2 are the fields of vapor and salt fluids, respectively; $L_1 + L_2$ is the field where these two fluids coexist. (*1*) Experiments without chlorine; (*2*) L_1 fluid; (*3*) $L_1 + L_2$ fluid; (*4*) $L_1 + L_2$ fluid, experiments with elevated chlorine contents of melts; and (*5*) L_2 fluid.

even in the presence of almost anhydrous homogeneous chloride melt (94–98 wt % MeCl in the initial fluid).

Table 1 presents some molar ratios of glasses, A/CNK = $Al_2O_3/(CaO + Na_2O + K_2O)$, NK/A = $(Na_2O + K_2O)/Al_2O_3$, ANC/S = (Al + Na + Ca)/Si, and ANCK/S = (Al + Na + Ca + K)/Si. The results of previous studies, e.g., [5, 7], suggest that these parameters control chlorine solubility in aluminosilicate melts of various compositions. According to [22], almost all our samples fall within the field of metaluminous compositions (A/CNK < 1 and NK/A < 1) and some of them from experiments with a salt or two-phase fluid approach subaluminous compositions (A/CNK ~ 1). Only two samples with glasses strongly depleted in calcium fall within the peraluminous field (A/CNK > 1).

From the four molar ratios presented in Table 1, two appeared to be the most appropriate for the construction of correlation dependencies, A/CNK and ANC/S. These integrated parameters adequately characterize the composition of melt in the system studied. The value A/CNK, which is the inverse of the agpaicity index, reflects excess alumina or alkali content relative to the feldspar component. The second parameter, ANC/S, shows the proportion of feldspar and quartz components in the composition. The use of NK/A for the interpretation of our experimental results might result in erroneous conclusions (e.g., Fig. 3 and explanation to it in the text). The diagrams constructed with the ratio ANCK/S showed dependencies similar to, but less clear than, those with ANC/S.

Figure 2 shows the chlorine content of melt as a function of A/CNK, which characterizes melt composition. Despite our effort to minimize variations in the compositions of experimental melts, A/CNK varied in our samples from 0.73 to 1.0 and higher (Table 1). Straight lines show distinct negative correlations (because melt compositions are enriched in alkalis and calcium) between chlorine and A/CNK. Line *1* shows chloride-saturated melts in the region of a vapor-dominated fluid, L_1. Line *2* approximates experimental melts with elevated chlorine contents (A/CNK from ~0.76 to 0.80). Line *3* shows experiments in the presence of two-phase or salt fluids (A/CNK from ~0.85 to 0.99 or higher). Chlorine content in melt increases with increasing excess of calcium, sodium, and potassium relative to the feldspar end-member. This type of dependency has been pointed out by many researchers [5]. Correlation lines *2* and *3* (Fig. 2) are probably related to two mechanisms of chlorine incorporation in the melt structure, which are discussed below.

Figure 3 shows chlorine content of melt as a function of NK/A. Two straight lines bounding the field of chlorine-bearing experiments illustrate a direct correlation between chlorine content and NK/A of melt. This dependency is in apparent contradiction with the results of previous studies [5], because the opposite dependency should be observed in melts with NK/A < 1. However, since our system also contains calcium, the melt compositions are enriched in total in sodium, potassium, and calcium relative to the feldspar end-member. The correct correlation dependencies can be obtained using the A/CNK ratios (e.g., Fig. 2).

Figure 4 shows chlorine content as a function of ANC/S, which varied in our experiments from ~0.4 to 0.54 (Table 1). The vertical line corresponds to line *1* in Fig. 2 and points out the constancy of ANC/S ~(0.46–0.47) in the region of vapor-dominated fluid (L_1, chlorine-undersaturated compositions). The horizontal line corresponds to line *3* in Fig. 2 and demonstrates that in the presence of two-phase and salt fluids, ANC/S in our experiments varied from ~0.40 to 0.45 (0.48) at a chlorine content of ~0.5–0.7 wt %. Line *2* emanates from the intersection of lines *1* and *3* and corresponds to experiments with high chlorine contents of melt and elevated ANC/S values of ~0.47–0.49.

Results of the Analysis of IR Spectra of Quenched Glass Samples

Table 2 shows the results of the IR spectral analysis of granodiorite glass samples, which are expressed as the fraction of six-membered rings in the sum of six- and four-membered rings. This fraction is referred to as the structural parameter α and varies in our samples within ~0.60–0.76. It should be noted that this parameter is conventional and not strictly quantitative. We are aware that rings in amorphous glass may be distorted in a random way. Probably, overlapping is possible. Part of angles in the distorted T–O–T bonds of four-membered rings could be equal to those of six-membered units. The abundance of five-membered rings is not adequately known. Therefore, α can be considered as a

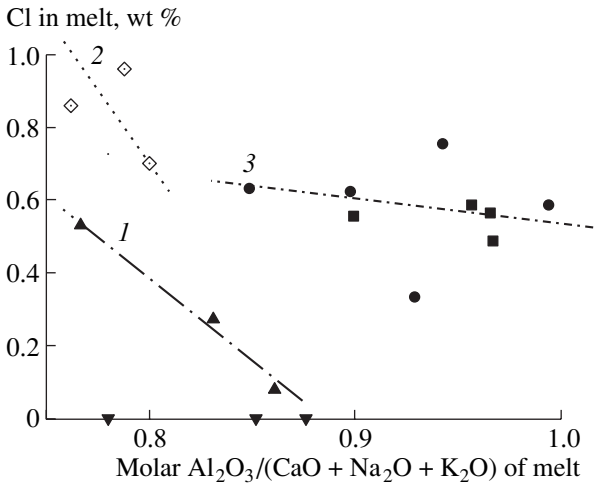

Fig. 2. Correlation of the chlorine content and the molar ratio $Al_2O_3/(CaO + Na_2O + K_2O)$ of melt. (*1*) Experiments in the field of vapor fluid (L_1) with melt undersaturated in chlorides; (*2*) experiments with elevated chlorine content of melt in the presence of two-phase fluid; and (*3*) experiments in the presence of two-phase and salt fluids. Other symbols are the same as in Fig. 1.

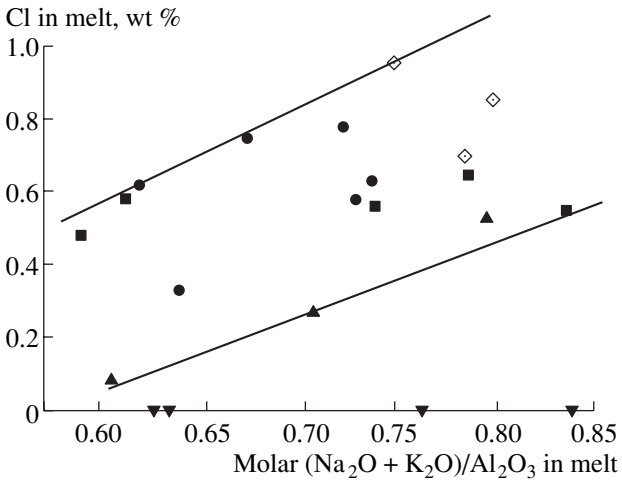

Fig. 3. Chlorine content of granodiorite melt as a function of the molar ratio $(Na_2O + K_2O)/Al_2O_3$. Two straight lines bound the field of chlorine-bearing experiments. Symbols are the same as in Fig. 1.

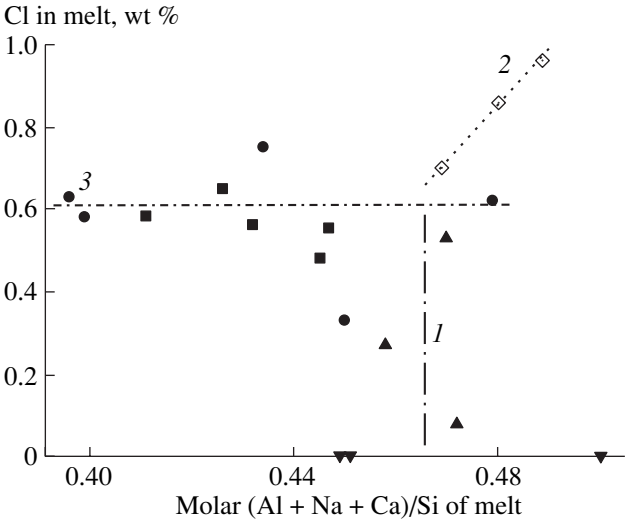

Fig. 4. Chlorine content of melt as a function of the molar ratio (Al + Na + Ca)/Si. Symbols are the same as in Figs. 1 and 2.

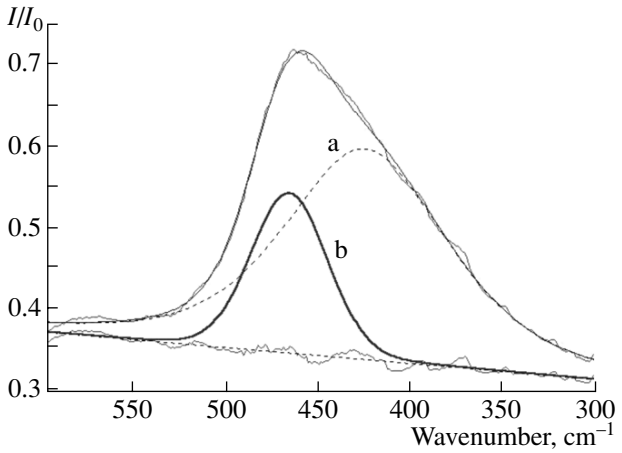

Fig. 5. An example of the spectrum of infrared absorption of chlorine-bearing hydrous glass. The spectrum is approximated by two symmetric contours corresponding to (a) six-membered (423 cm^{-1}) and (b) four-membered (465 cm^{-1}) rings. The lower lines are the base line and residue diagram.

relative parameter that reflects structural transformations rather than the absolute fractions of particular structural units.

Figure 5 shows an example of the approximation of the asymmetric band of the IR spectrum of chlorine-bearing hydrous glass by two symmetric contours corresponding to six- and four-membered rings. Figure 6 shows two histograms of distribution constraining the positions of vibration maxima corresponding to six- (average frequency of 423 cm^{-1}) and four-membered (465 cm^{-1}) rings in the IR spectra of all analyzed glasses from the results of approximation. Sykes and Kubicki [23] predicted frequencies of 480–490 cm^{-1} for the deformation vibrations of four-membered rings. Seifert *et al.* [24] reported an interval of 480–490 cm^{-1} for this band in dry glasses. Quartz glass shows a characteristic band at 437 cm^{-1} [25], which is higher than the value accepted by us for six-membered rings. This displacement could be due to the fact that part of the aluminum probably occurs in six-membered rings, which results in a decrease in the frequency of similar vibrations in four- and three-membered rings. The precision of measurements and approximation was assessed through the repeated measurements of other

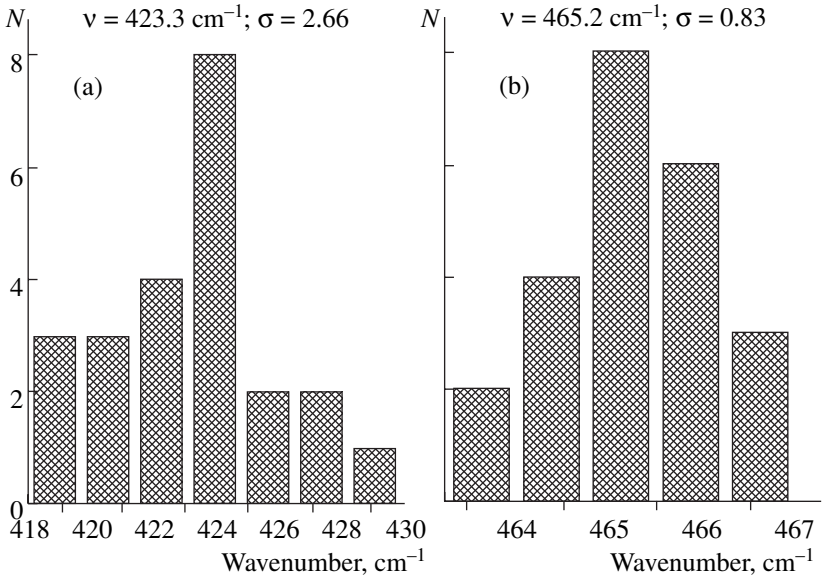

Fig. 6. Histograms characterizing the position of vibration maxima in the IR spectra of all analyzed glasses, which correspond, according to the results of approximation, to (a) six-membered (423 cm^{-1}) and (b) four-membered (465 cm^{-1}) rings.

parts of samples. The maximum deviation from the average value was ±0.02 (~3% rel.).

Figure 7 shows that the structural parameter α changes in a complex way with variations in the chlorine content of melt. The results can be approximated by two dependencies, which probably correspond to the two mechanisms of chlorine dissolution in the melt structure discussed below. First, an increase in the chlorine content of melt from 0 to ~0.65 wt % is accompanied by an increase in α, which is initially rather abrupt from ~0.64 to ~0.70 and more gradual from 0.70 to ~0.74. These changes correspond to the transition of four-membered feldspar elements of the aluminosilicate network into six-membered tridymite-like structural elements. Second, the results obtained for samples

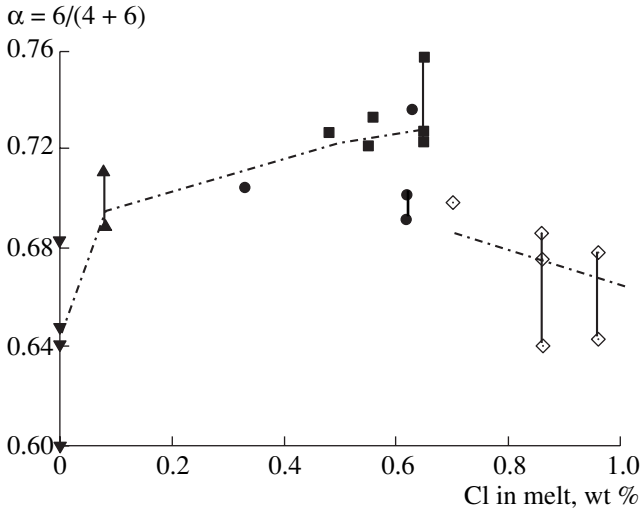

Fig. 7. Variations of the structural parameter α as a function of the chlorine content in granodiorite melt. Points corresponding to a single experiment are connected by vertical lines. Symbols are the same as in Fig. 1.

with "anomalously" high chlorine in melt, from ~0.70 to 0.96 wt %, reveal the opposite tendency. In these samples, the value of α declines to 0.66–0.70 and approaches the α value of chlorine-free quenched glasses.

In order to asses the influence of changes in the composition of granodiorite glass on the value of the structural parameter α from the data presented in Tables 1 and 2, correlation coefficients were calculated between the average values of α and various molar ratios and between α and concentrations of particular elements in glass composition. A significant correlation was found between α and A/CNK (R = +0.85), ANC/S (R = –0.95), SiO_2 (R = +0.88), and CaO (R = –0.69). Figure 8 shows variations in the structural parameter α as a function of A/CNK. It is seen that an increase in A/CNK from ~0.73 to 0.97 is accompanied by an increase in the fraction of six-membered rings. When A/CNK rises above one, α stabilizes at a level of ~0.73 and does not increase further. Thus, the excess of alkalis and calcium in melt composition stabilizes four-membered feldspar structural units (α decreases). Figure 9 shows changes in the value of α depending on the molar ratio ANC/S. It is seen that an increase in ANC/S from ~0.4 to ~0.54 is accompanied by a gradual α decrease; i.e., the fraction of four-membered rings increases in the structure of quenched glass.

Bulk H_2O Content and Concentrations of OH^- and Molecular Water in the Composition of Granodiorite Melt

Table 2 shows the results of the determination of H_2O speciation in granodiorite glasses, the ratio of OH^- group concentration to bulk water content (OH^-/H_2O), and the sum of chlorine and water contents, $\Sigma(Cl + H_2O_\Sigma)$.

Table 2. Structural characteristics and concentrations of different H_2O forms in granodiorite glasses

Run no.	$\alpha = 6/(4+6)$[1]*			Plate thickness[3]*, cm	ρ[4]*, g/l	OH^- absorbance	ε_{OH}[4]*, l/(mol cm)	H_2O_{mol} absorbance	ε_{H_2O}[4]*, l/(mol cm)	H_2O_Σ[5]*, wt %	OH^-[5]*, wt %	H_2O_{mol}[5]*, wt %	OH^-/H_2O_Σ[6]*	$\Sigma(Cl + H_2O_\Sigma)$[6]*
	I[2]*	II[2]*	III[2]*											
215	0.683													
223		0.602	bad spectrum	0.0195	2370	0.0484	1.09	0.0841	1.25	4.35	1.73	2.62	0.398	4.35
						0.0510		0.0880		4.57	1.82	2.75	0.399	4.57
				0.0194		0.049		0.094		4.71	1.76	2.95	0.374	4.71
224		0.647	0.640	0.0386	2370	0.0871	1.13	0.1613	1.30	3.96	1.52	2.44	0.384	3.96
						0.0878		0.1608		3.97	1.53	2.44	0.385	3.97
				0.0353		0.092		0.168		4.53	1.75	2.78	0.386	4.53
228		0.689	0.711	0.0251	2350	0.0652	1.19	0.1304	1.37	4.58	1.67	2.91	0.365	4.66
						0.0679		0.1296		4.63	1.74	2.89	0.376	4.71
216	0.640	0.686	0.675	–	2340	–	1.14	–	1.32	4.52	1.54	2.98	0.341	5.38
222		0.643	0.678	0.0123	2340	0.0268	1.13	0.0527	1.30	4.02	1.48	2.54	0.368	4.98
						0.0279		0.0553		4.21	1.55	2.66	0.368	5.17
						0.0298		0.0551		4.30	1.65	2.65	0.384	5.26
				0.011		0.028		0.051		4.48	1.73	2.75	0.386	5.44
234 (bubble-free)			0.698	0.02265	2340	0.061	1.16	0.105	1.34	4.44	1.78	2.66	0.401	5.14
230			0.721	0.0213	2335	0.0575	1.20	0.1083	1.38	4.58	1.74	2.84	0.380	5.13
			shift (419)			0.0574		0.1128		4.70	1.74	2.96	0.370	5.25
231			0.733	0.0155	2335	0.042	1.22	0.082	1.41	4.61	1.71	2.90	0.371	5.17
217 (Ca deficit)	0.758	0.722	0.727	–	2335	–	1.23	–	1.42	4.52	1.68	2.84	0.372	5.17
220			0.727	0.0287	2335	0.0800	1.24	0.1447	1.44	4.43	1.73	2.70	0.391	4.91
						0.0786		0.1480		4.46	1.70	2.76	0.381	4.94
				0.0285		0.084		0.148		4.61	1.83	2.78	0.397	5.09
225				0.0174	2335	0.051	1.27	0.098	1.48	4.72	1.78	2.94	0.377	5.30
218 (Ca deficit)	0.729		0.726											
235 (bubble-free)			0.736											
221		0.701	0.691	0.0223	2335	0.0611	1.22	0.1109	1.42	4.43	1.73	2.70	0.391	5.05
				0.0213		0.058		0.117		4.71	1.72	2.99	0.365	5.33
227			0.704	0.0128	2335	0.0318	1.23	0.0626	1.42	4.22	1.56	2.66	0.370	4.55
						0.0352		0.0627		4.39	1.73	2.66	0.394	4.72
				0.01275		0.0333		0.064		4.37	1.64	2.73	0.375	4.70

Note: [1]* Results of the analysis of IR spectra of quenched glass samples expressed as α, the ratio of six-membered rings to the sum of four- and six-membered rings (see text for more details).

[2]* Three sequentially conducted measurement series.

[3]* Thickness of plates prepared for the determination of water content in samples.

[4]* Glass density ρ used in the calculation of water content; ε_{OH} and ε_{H_2O} are the coefficients of molar excitation of OH^- and H_2O_{mol} calculated after [18].

[5]* Concentrations of different H_2O forms in glass samples: H_2O_Σ is the bulk content, OH^- is the content of OH^- groups, and H_2O_{mol} is the content of molecular water.

[6]* OH^-/H_2O_Σ is the ratio of the concentration of OH^- groups to the bulk water content; $\Sigma(Cl + H_2O_\Sigma)$ is the sum of chlorine and water contents in glass samples.

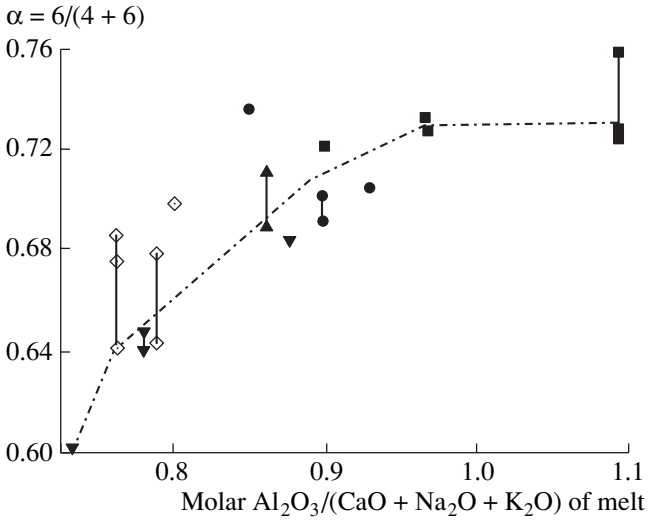

Fig. 8. Structural parameter α as a function of the molar ratio $Al_2O_3/(CaO + Na_2O + K_2O)$ in melt composition. Symbols are the same as in Figs. 1 and 7.

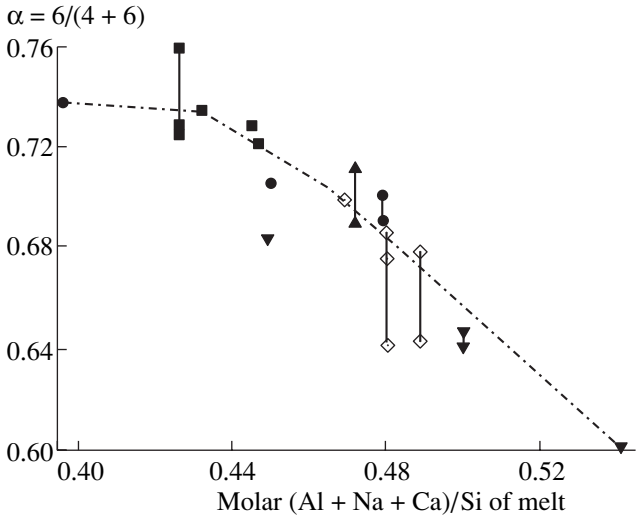

Fig. 9. Structural parameter α as a function of the molar ratio (Al + Na + Ca)/Si in melt composition. Symbols are the same as in Figs. 1 and 7.

The bulk water content in the experimental granodiorite glasses was determined as ~4.2–4.6 wt %.

Figure 10 shows the dependency of the bulk H_2O content in granodiorite glass on the molar ratio A/CNK. The data obtained can be divided conventionally into two groups similar to the above-discussed distinction with respect to the chlorine content of melt and the value of the structural parameter α as a function of A/CNK. Glasses enriched in alkalis and calcium (A/CNK = 0.73–0.80) show relatively low bulk water contents, ~4.2–4.5 wt % on average, whereas more aluminous compositions (A/CNK = 0.86–1.09) have slightly higher bulk water contents, ~4.5–4.6 wt %.

Figure 11 shows the fraction of OH^- groups in the bulk water content of quenched glasses. In general, there are no significant differences in the concentrations of both water forms dissolved in glasses. The distribution of water forms (hydroxyl and molecular water) in the quenched glasses does not depend on chlorine content and melt agpaicity and is approximately constant, $(OH^-/H_2O_\Sigma = 0.38 \pm 0.02)$.

There is a significant correlation between the chlorine content and the sum of chlorine and water in the composition of granodiotrite glass ($R = +0.90$). Figure 12 shows that the sum of chlorine and water contents, $\Sigma(Cl + H_2O_\Sigma)$, in glass samples is lowest in the chlorine-free experiments (~4.2–4.5 wt %), increases up to ~4.7 wt % in the experiments with presumably single-phase vapor and salt fluids, and attains a constant maximum level of ~5.1–5.3 wt % in all experiments with a two-phase fluid both with the normal and anomalously high chlorine content of glass. It can be suggested that in the experiments with anomalously high chlorine content, water and chlorine compete with each other for identical structural positions in the melt.

DISCUSSION

Correlation Analysis

The system that was experimentally studied is multicomponent, and, although it is a model, it is too complex to be analyzed on the basis of the above-described pair correlation relationships. Because of this, the data obtained on the structure and composition of granodiorite glass samples were described by a multiple linear regression model:

$$\alpha = 0.3216 + 0.3177(A/CNK) + 0.0179C_{H_2O} + 0.0177C_{Cl}. \quad (3)$$

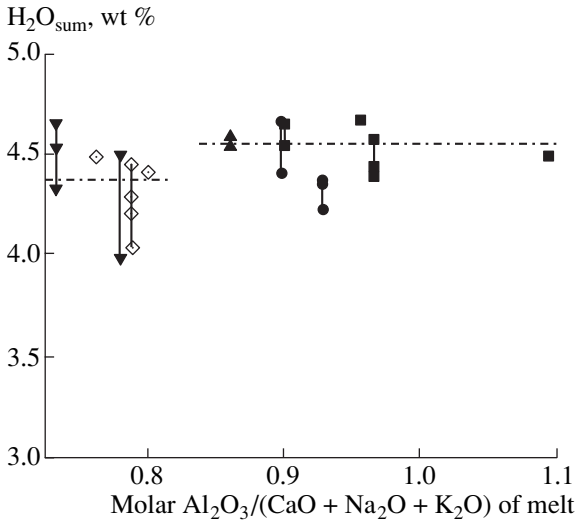

Fig. 10. Bulk water content as a function of the molar ratio $Al_2O_3/(CaO + Na_2O + K_2O)$ in granodiorite melt. Symbols are the same as in Figs. 1 and 7.

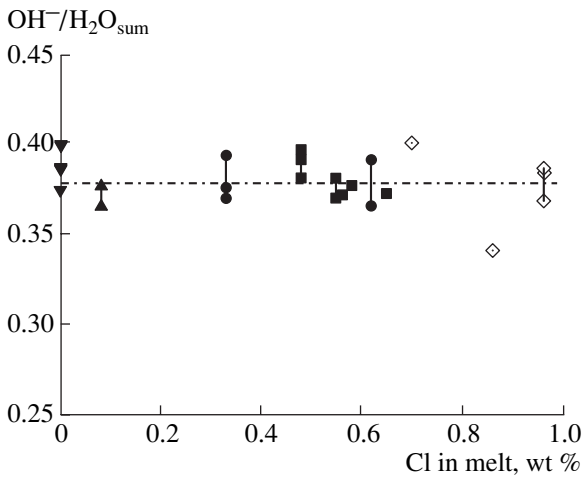

Fig. 11. Ratio of the concentration of OH^- groups to the bulk water content of granodioritic melt as a function of the chlorine concentration of glass. Symbols are the same as in Figs. 1 and 7.

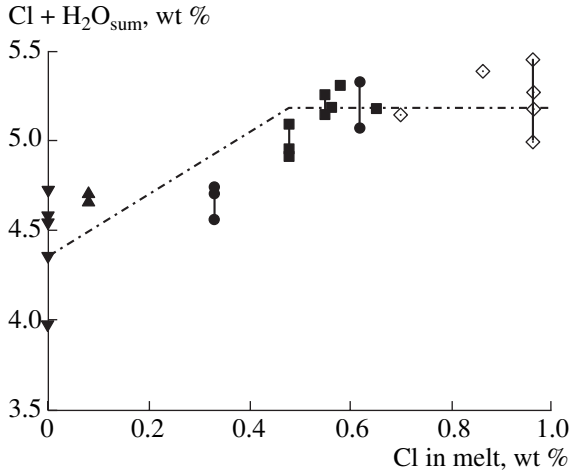

Fig. 12. Sum of H_2O and Cl contents of granodiorite glass as a function of the chlorine concentration of the glass. Symbols are the same as in Figs. 1 and 7.

The correlation coefficient is $R = +0.87$ (Fig. 13).

A multiple linear regression model for a set of random values (in our case, for the structural parameter α, water content, chlorine content, and molar ratio A/CNK) is characterized by the multiple correlation coefficient R. It shows the degree of connection between the variations of α and parameters that were taken as independent random values in the linear regression function:

$$\alpha - \bar{\alpha} = a_1(\text{A/CNK}) + a_2 C_{H_2O} + a_3 C_{Cl}. \qquad (4)$$

If the parameter α is strictly defined by the values of independent parameters, $R = 1$. If they are absolutely independent, $R = 0$.

All the data from Tables 1 and 2 were used for regression analysis. The whole data population shows a relatively high R of 0.87, which suggests a strong correlation between the parameters under consideration. It can be pointed out that the values of the coefficients $a_2 = a_{H_2O}$ and $a_3 = a_{Cl}$ are similar in order of magnitude and close to the coefficient of proportionality between the water content and the structural parameter α of granitic melt [13]. On the other hand, a_{H_2O} and a_{Cl} are much smaller than $a_1 = a_{A/CNK}$, which characterizes the general composition of the melt. Taking into account the dependence of the molar ratio A/CNK on the concentrations of cations, it can be shown that the influence of sodium and potassium on the structural parameter α is of the same order of magnitude as the influence of chlorine and water.

Discussion of Experimental Results

It was expected that, with increasing chloride content of fluid phases, the Cl concentration of granodioritic melt would increase in the presence of a homogeneous vapor fluid, be constant in the region of a two-phase fluid, and remain at the same level or increase in the presence of a homogeneous salt fluid. The concentration of H_2O in the melt will be constant in the case of a homogeneous vapor or two-phase fluid and decrease with decreasing water activity in the region of a single-phase salt fluid. The dependencies obtained are only partially consistent with these regularities, which were reported by Webster and other researchers [3–10].

Our experimental results revealed a region of anomalously high chlorine solubility in granodioritic melt

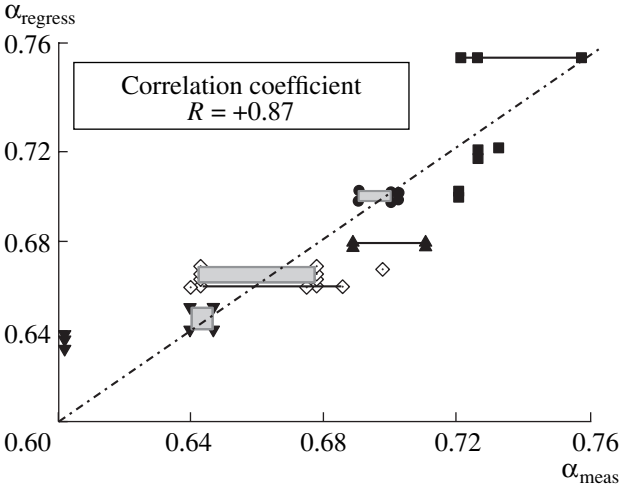

Fig. 13. Results of the multiple linear regression of the dependence of the structural parameter α on A/CNK, water content, and chlorine content in the composition of quenched granodiorite glass. Points corresponding to a single experiment are connected by lines or marked by rectangles. Other symbols are the same as in Fig. 1.

(up to 0.9–1.0 wt %) in the presence of a two-phase fluid with relatively low bulk MeCl concentration, ~7–11 wt %. More logically, the maximum on the chlorine solubility curve might have been expected in the region of a single-phase fluid. A decrease and approximate constancy are reasonable at the transition into the two-phase region. However, in accordance with [19–21], it seems improbable that at the *P–T* parameters of our experiments the decomposition of aqueous chloride fluid into two phases occurred at MeCl concentrations no lower than 10 wt %. We believe that this maximum chlorine concentration is related to differences in melt composition (increase in agpaicity: A/CNK decreases from 0.9–1.09 to 0.76–0.80, while ANC/S increases from 0.41–0.48 to 0.47–0.54). However, it is possible that the differences in melt composition are related in turn to fluid–melt interaction. These changes in melt composition exert a more pronounced influence on chlorine solubility than on water solubility. Changing the composition of initial solution, we attempted to minimize the difference in the compositions of quenched glasses, but the remaining variations probably affected the results.

The bulk water content of granodiorite glass is almost invariant within the whole compositional range (~4.2–4.6 wt %) and practically independent of the composition of fluid coexisting with the melt.

It is difficult to describe rigorously the coupling of water and chlorine solubilities in magmatic melt, because solubility depends on the properties of fluid, the activity of its components, melt composition, and a number of other parameters. It was shown above that the total set of experimental results is characterized by a significant pair correlation between chlorine content and the sum of chlorine and water in the composition of granodiorite glasses. Water concentration is approximately constant (~4.5–4.6 wt %) in the melts with normal chlorine contents (lower than ~0.7 wt %) and independent of chlorine solubility. The melts with anomalously high chlorine contents contain ~4.2–4.5 wt % of water, and their chlorine and water concentrations are inversely proportional; i.e., chlorine competes with water, in them. It can be supposed that in such a case, dissolution of water and chlorine in granodiorite melt is accompanied by their interaction with alkali earth or alkali metals through similar mechanisms.

Our experimental samples can be divided into two groups using the following four criteria: differences in melt composition (A/CNK and ANC/S), chlorine content of melt, bulk water content of melt, and the structural parameter α.

No.	A/CNK	ANC/S	Structural parameter $\alpha = 6/(4 + 6)$	Chlorine content of melt	Water content of melt
Group I	0.73–0.80	0.47–0.54	0.60–0.70	0.7–0.96% and Cl-free experiments	~4.2–4.5%
Group II	0.90–1.09	0.41–0.48	0.70–0.74	0.48–0.65% (0.33%)	~4.5–4.6% (4.3%)

The first group comprises glasses with anomalously high chlorine contents and from experiments without chlorine, which are enriched in Ca, Na, and K. The second group includes glasses from remaining experiments. For experiment 227 with a concentrated salt phase, numerals in parentheses show low concentrations of chlorine and water deviating from the general trend. It should be noted that the difference in water content between the glasses of these two groups is within the scatter of our results and this effect must be confirmed by additional data.

Two Possible Mechanisms of Chlorine Dissolution in Granodiorite Melt

It is known that chlorine is bonded in the melt structure only to network-modifying cations (Na, K, Ca, Fe, etc.) in contrast to fluorine, which can also interact with the network-forming elements (Si and Al). Granodioritic melt is composed mainly of tridymite (six-membered rings) and feldspar (four-membered rings) structural units. The feldspar structural units are stabilized by cations of alkali and alkali earth metals bonded with them. Two alternative hypotheses can be proposed for chlorine dissolution in granodioritic melt.

According to one hypothesis, all the data, except for the experiments with anomalously high chlorine contents, can be interpreted in the context of the structure of polymerized granitic and granodioritic melts. Metal chlorides can probably form interstitial solutions with the aluminosilicate network (Fig. 14). Chlorides are preferentially incorporated in the areas with a local medium-range order structure composed of six-membered tridymite-like aluminosilicate rings, which is consistent with the above-described IR spectroscopic data (Fig. 7; Fig. 2, line *3*). That is, the decomposition of feldspar structural units and release of network-modifiers in general promote chlorine dissolution in the melt. According to [26], the albite end-members (structural elements of melt) are unstable in silicic melt and decompose in part into the nepheline and quartz end-members. Chlorine and water can be incorporated into

nepheline components forming the sodalite end-member, which can be imagined as a local environment of chlorine in melt proceeding from the structure of NaCl solid solution in aluminosilicate. The structure of sodalite, $6NaAlSiO_4 \cdot 2NaCl$, is a hollow "lantern" composed of six-membered rings (with a T–O–T angle of 138.5° similar to tridymite) forming four-membered junctions with the same angles of the T–O–T bonds. The chlorine ion sits within the cavity and is tetrahedrally coordinated by Na ions. The density of the compound is about 2.3, which is close to the density of hydrous silicic melt. Thus, the nearest environment of chlorine in melt is probably formed by alkali and alkali earth cations. In addition, they interact with the aluminosilicate network compensating the excess charges of oxygen of the rings. The example of sodalite shows that the whole construction may be symmetric (cubic system), which does not allow us to allege a specific connection between chlorine and any particular metal ion. In addition to sodium, calcium may occur in the structure of sodalite (lazurite), whereas the incorporation of potassium in such a structure is less probable. Potassium feldspar is one of the most stable feldspars, in which the large potassium atom resides in the hollow that could have been occupied by chlorine or water. This is consistent with the experimental data of Chevychelov and Suk [27], who demonstrated that chlorine solubility in potassium-rich aluminosilicate melt is lower than that in calcium- and sodium-rich compositions.

On the other hand, chlorine may occur in melt in two positions: either in the coordination sphere of the cations that almost do not interact with the network or in the coordination sphere of the cations that do not lose such a connection. Chlorine bonded with a released cation forms as if a microcluster of the salt phase. Anfilogov *et al.* [28] described transitions from salt solutions in a silicate component on the molecular level through microclusters to liquid immiscibility. The true solubility of chlorides in silicate melts is rather low and controls chlorine solubility, for example, in the form of NaCl. On the other hand, divalent calcium can form salts of the oxychloride type, ($CaClO^-$), where oxygen is connected with the feldspar structural unit. Chlorine bonded through calcium with the network occupies the second structural position, which is filled in addition to the pure salt one. Water dissolution in melt containing anorthite structural components can also be accompanied by partial hydration of calcium. Chlorine and hydroxyl may compete for this position. It is conceivable that, along with the first mechanism, the second mechanism of chlorine dissolution begins working at anomalous high chlorine solubility (~0.7–0.96) in the system studied. In such glasses, the structural parameter α is equal to 0.66–0.70, i.e., the number of feldspar structural units in these melts is higher than that of chlorine-bearing melts from other experiments (Fig. 7; Fig. 2, line *2*). According to the crystal chemistry of feldspars, Ba and, to a lesser extent, Sr can play a role similar to that of Ca. Other divalent cations, such as Fe and Mg, do not enter the feldspar structure and are probably not bonded in melt with feldspar structural units. Because of this, their role in the positioning of chlorine in the melt structure may be different.

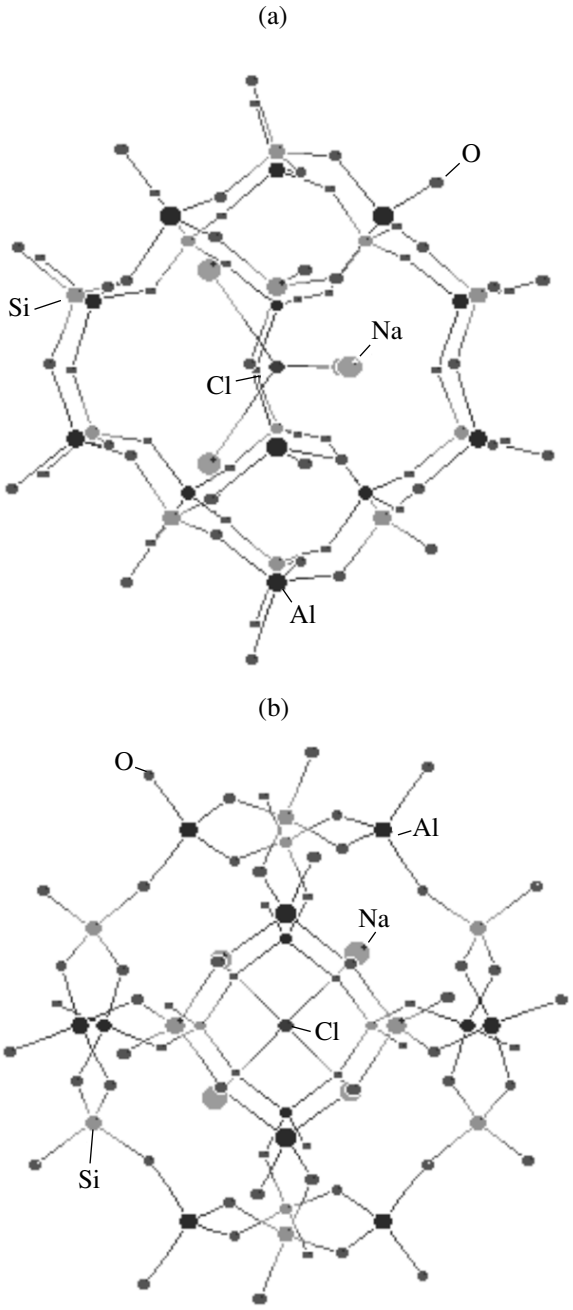

Fig. 14. Possible position of chlorine in the structure of polymerized granite–granodiorite melt. (a) 110- and (b) 010-projections of an individual "lantern" of sodalite structure with a tetrahedron of Na ions surrounding Cl^- in the center. This picture was prepared using the program MolDraw (4.0, 1989) designed by P. Ugliengo, G, Borzani, D. Viterbo, and G. Chiari.

A more detailed description of different structural positions of Ca in melt can be obtained by means of

NMR investigations using the stable rare isotope ^{43}Ca. For instance, Zavel'skii and Salova [29] determined two positions of ^{23}Na in sodium silicate glass. The more symmetric position was correlated with detached sodium, while the less symmetric was interpreted as being connected with the network. The second position changes into the first one as the water content increases.

CONCLUSION

(1) At $P = 1$ kbar and $T = 1000°C$, chlorine solubility in granodiorite melt is ~0.50–0.65 wt % at a fluid chloride salinity higher than ~15 wt %. The bulk water content of granodiorite glass is ~4.2–4.6 wt %. A region of anomalously high chlorine solubility (up to 0.9–1.0 wt %) was observed at a total salinity of the two-phase fluid of ~7–11 wt % of MeCl. We believe that it is related to variations in melt composition (molar ratio A/CNK decreases from 0.9–1.09 to 0.76–0.80, while ANC/S increases from 0.41–0.48 to 0.47–0.54). These differences in melt composition exert a stronger influence on chlorine solubility than on water solubility.

(2) The concentrations of water and chlorine in melt are essentially independent of each other at Cl contents lower than ~0.7 wt %. Only at anomalously high chlorine contents did the concentrations of chlorine and water become inversely proportional. It is reasonable to suppose that chlorine begins competing with water for similar structural position in the melt.

(3) The data obtained allowed us to reveal a good multiple correlation ($R = +0.87$) between the structural parameter α and melt composition characteristics, (A/CNK), water content, and chlorine content. It was found that differences in melt composition (A/CNK and ANC/S) exert a stronger influence on the value of α in comparison with the effect of water and chlorine contents of the melt. This is supported by the fact that the whole set of results is characterized by good pair correlations between the structural parameter α and A/CNK, ANC/S, and SiO_2 and CaO concentrations.

(4) Two alternative mechanisms were proposed for chlorine dissolution in granodiorite melt. At concentrations of ~0.50–0.65 wt %, chlorine probably enters the structure of polymerized melt during the decomposition of feldspar structural elements and formation of sodalite ones. At higher contents of ~0.70–0.96 wt %, chlorine could also be connected through divalent calcium with the feldspar structural elements. The absence of salt phases in the glasses was ascertained by TEM investigations at a magnification of 100 000.

ACKNOWLEDGMENTS

The authors are grateful to P. Armienti (University of Pisa, Italy), who determined the water contents in our samples, V.I. Nikolaichik (Institute of Microelectronic Technology and Ultra-High-Purity Materials, Russian Academy of Sciences, Chernogolovka, Moscow oblast), who carried out TEM investigations, and A.V. Chichagov (Institute of Experimental Mineralogy, Russian Academy of Sciences) for the structural data on sodalite, which enabled the construction of the graphical representation of the mineral structure. The authors thank K.I. Shmulovich, E.S. Persikov, G.P. Zaraiskii (Institute of Experimental Mineralogy, Russian Academy of Sciences), E.B. Lebedev (Vernadsky Institute of Geochemistry and Analytical Chemistry, Russian Academy of Sciences), and E.N. Gramenitskii (Moscow State University) for comprehensive suggestions and comments and discussion of the manuscript. This study was financially supported by the Russian Foundation for Basic Research, project nos. 99-05-65439, 99-05-64106, 00-15-98504, and 01-05-64837.

REFERENCES

1. Marakushev, A.A., Gramenitskii, E.N., and Korotaev, M.Yu., Petrological Model of Endogenic Ore Formation, *Geol. Rudn. Mestorozhd.,* 1983, no. 1, pp. 3–20.
2. Candela, P.A. and Piccoli, P.M., Model Ore-Metal Partitioning from Melts into Vapor and Vapor–Brine Mixtures, in *Magmas, Fluids, and Ore Deposits*, Thompson, J.F.H., Ed., Mineral. Assoc. Can., 1995, pp. 107–127.
3. Malinin, S.D. and Kravchuk, I.F., Chlorine Behavior in the Equilibria of Silicate Melt with Water-Chlorine Fluid, *Geokhimiya*, 1995, no. 8, pp. 1110–1130.
4. Webster, J.D., Exsolution of Magmatic Volatile Phases from Cl-Enriched Mineralizing Granitic Magmas and Implications for Ore Metal Transport, *Geochim. Cosmochim. Acta*, 1997, vol. 61, no. 5, pp. 1017–1029.
5. Chevychelov, V.Yu., Calcium Effect on Chlorine Solubility in Fluid-Saturated Granitic Magmas, *Geokhimiya*, 1999, no. 5, pp. 522–535.
6. Shinohara, H., Iiyama, J.T., and Matsuo, S., Partition of Chlorine Compounds between Silicate Melt and Hydrothermal Solutions: I. Partition of NaCl and KCl, *Geochim. Cosmochim. Acta*, 1989, vol. 53, no. 10, pp. 2617–2630.
7. Webster, J.D., Kinzler, R.J., and Mathez, E.A., Chloride and Water Solubility in Basalt and Andesite Melts and Implications for Magmatic Degassing, *Geochim. Cosmochim. Acta*, 1999, vol. 63, no. 5, pp. 729–738.
8. Webster, J.D. and Rebbert, C.R., Experimental Investigation of H_2O and Cl^- Solubility in F-Enriched Silicate Liquids: Implications for Volatile Saturation of Topaz Rhyolite Magmas, *Contrib. Mineral. Petrol.*, 1998, vol. 132, no. 2, pp. 198–207.
9. Webster, J.D., Chloride Solubility in Felsic Melts and the Role of Chloride in Magmatic Degassing, *J. Petrol.*, 1997, vol. 38, no. 12, pp. 1793–1807.
10. Webster, J.D., Fluid–Melt Interactions Involving Cl-Rich Granites: Experimental Study from 2 to 8 kbar, *Geochim. Cosmochim. Acta*, 1992, vol. 56, pp. 659–678.
11. Mysen, B. and Frantz, J., Structure and Properties of Alkali Silicate Melts at Magmatic Temperatures, *Eur. J. Mineral.*, 1993, vol. 5, pp. 393–407.
12. Bykov, V.N., Local Structure of Silicate and Natural Glasses and Melts: Vibration Spectroscopic Studies, *Abstract of Doctoraal (Chem.) Dissertation*, Moscow: Inst. Mineral., Ural. Div. Russ. Acad. Sci., 2000.

13. Simakin, A.G., Salova, T.P., Epel'baum, M.B., and Bondarenko, G.V., The Effect of Water on the Structure of Aluminosilicate Melt, *Geokhimiya*, 1998, no. 8, pp. 861–864.
14. Sykes, D., Marians, J.C., and Burdett, J., Geometric Constraints: A Refined Model for the Structure of Silica Glass, *J. Non-Cryst. Solids*, 1990, vol. 124, pp. 1–21.
15. Zotov, N. and Keppler, H., The Influence of Water on the Structure of Hydrous Sodium Tetrasilicate Glasses, *Am. Mineral.*, 1998, vol. 83, pp. 823–834.
16. Hamilton, D.L. and Henderson, C.M.B., The Preparation of Silicate Compositions by a Gelling Method, *Mineral. Mag*, 1968, vol. 36, no. 282, pp. 832–838.
17. Roy, R., Aids in Hydrothermal Experimentation, *J. Am. Ceram. Soc.*, 1956, vol. 39, pp. 145–146.
18. Ohlhorst, S., Behrens, H., and Holtz, F., Compositional Dependence of Molar Absorptivities of Near-Infrared OH^- and H_2O Bands in Rhyolitic to Basaltic Glasses, *Chem. Geol.*, 2001, vol. 174, pp. 5–20.
19. Bodnar, R.J., Burnham, C.W., and Sterner, S.M., Synthetic Fluid Inclusions in Natural Quartz. III. Determination of Phase Equilibrium Properties in the System H_2O–NaCl to 1000°C and 1500 bars, *Geochim. Cosmochim. Acta*, 1985, vol. 49, pp. 1861–1873.
20. Chou, I.M., Phase Relations in the System NaCl–KCl–H_2O. III. Solubility of Halite in Vapor-Saturated Liquids above 445°C and Determinations of Phase Equilibrium Properties in the System NaCl–H_2O to 1000°C and 1500 bars, *Geochim. Cosmochim. Acta,* 1987, vol. 51, pp. 1965–1975.
21. Shmulovich, K.I., Tkachenko, S.I., and Plyasunova, N.V., Phase Equilibria in Fluid Systems at High Pressures and Temperatures, in *Fluid in the Crust: Equilibrium and Transport Properties*, Shmulovich, K.I. *et al.*, Eds., London: Chapman and Hall, 1995, pp. 193–214.
22. Johannes, W. and Holtz, F., *Petrogenesis and Experimental Petrology of Granitic Rocks. Minerals and Rocks*, Berlin: Springer-Verlag, 1996.
23. Sykes, D. and Kubicki, J.D., Four-Member Rings in Silica and Aluminosilicate Glasses, *Am. Mineral.,* 1996, vol. 81, pp. 265–272.
24. Seifert, F.A., Mysen, B.O., and Virgo, D., Three-Dimensional Network Structure of Quenched Melts (Glass) in the Systems SiO_2–$NaAlO_2$, SiO_2–$CaAl_2O_4$, and SiO_2–$MgAl_2O_4$, *Am. Mineral.*, 1982, vol. 67, pp. 696–717.
25. Matson, D., Sharma, S., and Philpotts, J., Ramman Spectra of Some Tectosilicates and of Glasses along the Orthoclase–Anorthite and Nepheline Joins, *Am. Mineral.*, 1986, vol. 71, pp. 694–704.
26. Simakin, A.G. and Rincon, J.M., Structural Thermodynamic Model of the Melt in the System Ab–Q, *Phys. Chem. Glass,* 2002 (in press).
27. Chevychelov, V.Yu. and Suk, N.I., The Effect of Magma Composition on the Solubility of Metal Chlorides under Pressure of 0.1–3.0 kbar, *Petrologiya,* 2003, no. 1 (in press).
28. Anfilogov, V.N., Bobylev, I.B., Anfilogova, G.I., and Zyuzeva, N.A., *Stroenie i svoistva silikatno-galogenidnykh rasplavov* (The Structure and Properties of Silicate–Halide Melts), Moscow: Nauka, 1990.
29. Zavelsky, V.O. and Salova, T.P., The Role of Sodium in the Interaction of Sodium–Silicate Melt and Aqueous Fluid (NMR ^1H and ^{23}Na), *Geokhimiya*, 2001, no. 8, pp. 829–835.